Elastic Scattering of Polarized 10-Mev Protons by Complex Nuclei*

L. Rosen, J. E. Brolley, Jr., and L. Stewart
Los Alamos Scientific Laboratory, University of California, Los Alamos, New Mexico
(Received September 9, 1960)

A systematic investigation has been carried out on the angular dependence of the polarization in the elastic scattering of 10-Mev protons by complex nuclei. Strong polarization effects, which vary smoothly with scattering angle and atomic number of target nucleus, appear to be a general feature of the scattering process. All the data are fitted reasonably well by a 5-parameter "optical model potential" (containing a spin-orbit term) in which the only variable is the $A^{\frac{1}{3}}$ dependence of the radius. The strength of the spin-orbit term required to account for the polarization is approximately the same as has been postulated in the shell model.

I. INTRODUCTION

THE past decade has seen an intensive theoretical and experimental effort aimed at discovering a phenomenological model which unambiguously describes the interaction of intermediate-energy nucleons with complex nuclei.[1] (For purposes of the present discussion we define intermediate energies as being of the order of the energies which bind nucleons to nuclei.) One could then proceed to find the physical basis for the model and, hopefully, relate it to forces inferred from nucleon-nucleon studies. The search for a model in which the target nucleus is replaced by a potential has been greatly stimulated and influenced by the success of the shell model[2] in describing the systematics of ground states and of low-lying levels in terms of the configurations of individual nucleons moving freely in a potential representing the rest of the nucleus.

The time-honored source of information about the nuclear potential, as well as about the range of nuclear forces, is the scattering of nucleons by atomic nuclei. Systematic studies with protons over a large range of elements were first performed by Cohen and Neidigh[3] who found that the angular dependence of the elastic scattering of 22-Mev protons by complex nuclei is characterized by a diffraction-like pattern. This pioneering work was soon followed by equally comprehensive and more sophisticated studies at other energies.[4]

All of the above experiments yielded data which follow the same pattern. The more precise the data, the sharper are the maxima and minima in the angular

dependence of the differential cross sections; furthermore, the maxima and minima occur at the angles predicted by the elementary theory of diffraction and their positions are found to change smoothly with nuclear radius and proton energy.

The earliest attempts[5] to interpret these data utilized an optical model[6] in which the nucleus is replaced by a complex square-well potential of the form

$$V(r) = U + V + iW.$$

Here U represents the electrostatic potential, assumed to be that of a uniformly charged sphere, V relates to the cross section and angular distribution for elastic scattering and is analogous to the shell model potential which determines the nucleon configuration assignments, and the imaginary term takes account of non-elastic processes. It has been observed that a crude analogy to $V + iW$ is the complex index of refraction which one uses to describe the scattering of light by a partially opaque body.

Although the square well representation was not completely devoid of success, it was soon discovered by Woods and Saxon[7] that much better fits to experimental data could be obtained by using a potential well with sloping sides and rounded edges. They proposed a radial dependence for both the real and imaginary parts of the potential given by

$$\rho(r) = \left[1 + \exp\left(\frac{r-R}{a}\right)\right]^{-1}, \qquad (1)$$

where R is the mean nuclear radius and a is the so-called diffuseness parameter which determines the gradient of the potential at the surface of the nucleus. $\rho(r)$ may be thought of as representing the density distribution of nucleons in the nucleus. Such interaction potentials have been used with considerable success by a number of authors.[8]

* Work performed under the auspices of the U. S. Atomic Energy Commission.

[1] For a review of the recent literature on phenomenological analyses, see H. Feshbach, *Annual Review of Nuclear Science* (Annual Reviews, Inc., Palo Alto, 1958), Vol. 8, p. 49.

[2] E. Feenberg and K. C. Hammack, Phys. Rev. **75**, 1877 (1949); M. G. Mayer, Phys. Rev. **78**, 16 (1950); O. Haxel, J. H. D. Jensen, and H. E. Suess, Z. Physik **128**, 295 (1950). A. V. Savich, Soviet Phys.—JETP **3**, 400 (1956).

[3] B. L. Cohen and R. V. Neidigh, Phys. Rev. **93**, 282 (1954).

[4] I. E. Dayton and G. Schrank, Phys. Rev. **101**, 1358 (1956); B. B. Kinsey and T. Stone, Phys. Rev. **103**, 975 (1956); N. M. Hintz, Phys. Rev. **106**, 1201 (1957); G. W. Greenlees, L. G. Kuo, and M. Petravić, Proc. Roy. Soc. (London) **A243**, 206 (1957); W. F. Waldorf and N. S. Wall, Phys. Rev. **107**, 1602 (1957). For a complete bibliography of proton elastic-scattering measurements at intermediate energies, see M. K. Brussel and J. H. Williams, Phys. Rev. **114**, 525 (1959).

[5] R. E. Le Levier and D. S. Saxon, Phys. Rev. **87**, 40 (1952).

[6] H. A. Bethe, Phys. Rev. **57**, 1125 (1940); S. Fernbach, R. Serber, and T. B. Taylor, Phys. Rev. **75**, 1352 (1949).

[7] R. D. Woods and D. S. Saxon, Phys. Rev. **95**, 577 (1954); **101**, 506 (1956).

[8] M. A. Melkanoff, J. S. Nodvik, D. S. Saxon, and R. D. Woods, Phys. Rev. **106**, 793 (1957); A. E. Glassgold, W. B. Cheston, M. L. Stein, S. B. Schuldt, and G. W. Erickson, Phys. Rev. **106**, 1207 (1957).

In the meantime parallel developments had transpired under the impetus of attempts to describe the interaction of intermediate-energy neutrons with complex nuclei. The extensive experiments of the Wisconsin Group[9] on total neutron cross sections over the energy range 0.1–3 Mev showed that these cross sections did not follow the shape predicted by the compound nucleus (strong interaction) concept. They observed gross structure which was unrelated to individual resonances in the compound nucleus and which shifted more or less systematically to lower energies with increasing radius of target nucleus. These observations, together with other evidence which, by now, was placing severe strain on the strong-coupling model, led Feshbach, Porter, and Weisskopf[10] to propose a weak-interaction description of the energy exchange between neutron and target nucleus. This description relaxed the previous requirement that a neutron which enters a nucleus must have its motion immediately and intimately coupled with those of all the other nucleons.

In its earliest version, this so-called "cloudy crystal ball" model replaced the target nucleus by a complex square well which acts upon the incident neutrons. Since it averaged over resonances, the model could at most predict the cross sections for compound nucleus formation and for differential elastic (potential) scattering and it did this surprisingly well. However, there remained difficulties with the description of complete angular distributions for elastic scattering and, perhaps more important, the model did not predict compound nucleus formation cross sections as large as the observed nonelastic collision cross sections.

Diffusing the edges of the potential well[11] helped to alleviate the above difficulties, but some discrepancies still remained, especially with the differential cross section for elastic scattering through large angles. In order to resolve these, two further changes were made in the optical model potential. The first consisted of changing the form factor for the imaginary part of the potential to a Gaussian centered at the nuclear surface,[12] i.e.,

$$q(r) = \exp\{-[(r-R)/b]^2\}. \qquad (2)$$

The second involved the addition of a spin-orbit term to the optical potential, just as had been done to fit elastic scattering and polarization data at high energies. The form of the potential which now emerged appeared

quite adequate to describe,[13] in complete detail, a whole series of elastic neutron cross-section experiments.[14]

Rather independently of the above developments, the scattering of intermediate energy protons in a spin-orbit potential now began to receive theoretical attention.[15] The original idea for adding a spin-orbit term to the optical model potential can be traced to Fermi[16] who suggested that the polarization observed in high-energy proton-nucleus scattering might be related to the spin-orbit coupling assumed in the shell model. It will be recalled that one of the basic postulates of this model is that the nuclear potential which describes the motion of a particle in the effective field of the parent nucleus is composed, not only of a central component, but also of a strong spin-orbit component. The latter accounts, for example, for the experimental evidence that nucleonic orbits with spin parallel to the orbital angular momentum are depressed in energy relative to those in which spin and orbital momentum are oppositely directed. Specifically, Fermi proposed a non-central spin-orbit term proportional to the gradient of the central potential, in analogy with the Thomas precession term in atomic physics. More recently, Riesenfeld and Watson[17] have shown, rather more formally, that such a surface term is indeed the way in which spin-orbit coupling would most likely manifest itself. Additional evidence for the reality of a spin-orbit potential-energy term at intermediate energies was provided by a number of experiments[18] which yielded polarizations in the elastic scattering of neutrons from complex nuclei. However, the measured polarizations were small, the uncertainties large, and the number of determinations few. Furthermore, in view of the rather low incident energy, the observed polarizations could have been due to isolated resonance effects in the compound nucleus.

The evidence cited thus far argued for the inclusion of a spin-orbit term in the optical potential at intermediate energies. However, there was some weighty evidence to the contrary. Since spin-orbit coupling appears to play such an important part in bound nuclei, its effect should be manifest more strongly as the energy of an incident proton approaches that of the last proton inside the target nucleus. However, measurements of

[9] H. H. Barschall, Phys. Rev. 86, 431 (1952); D. W. Miller, R. K. Adair, C. K. Bockelman, and S. E. Darden, Phys. Rev. 88, 83 (1952).

[10] H. Feshbach, C. E. Porter, and V. F. Weisskopf, Phys. Rev. 96, 448 (1954).

[11] J. R. Beyster, M. Walt, and E. W. Salmi, Phys. Rev. 104, 1319 (1956); F. E. Bjorklund, S. Fernbach, and N. Sherman, Phys. Rev. 101, 1832 (1956).

[12] F. E. Bjorklund, S. Fernbach, and N. Sherman, Phys. Rev. 101, 1832 (1956); G. Culler, S. Fernbach, and N. Sherman, Phys. Rev. 101, 1047 (1956).

[13] F. E. Bjorklund and S. Fernbach, Phys. Rev. 109, 1295 (1958).

[14] J. H. Coon, R. W. Davis, H. E. Felthauser, and D. B. Nicodemus, Phys. Rev. 111, 250 (1958); M. H. MacGregor, W. P. Ball, and R. Booth, Phys. Rev. 111, 1155 (1958); S. Berko, W. D. Whitehead, and B. C. Groseclose, Nuclear Phys. 6, 210 (1958).

[15] G. W. Erickson and W. B. Cheston, Phys. Rev. 111, 891 (1958).

[16] E. Fermi, Nuovo cimento 11, 407 (1954).

[17] W. B. Riesenfeld and K. M. Watson, Phys. Rev. 102, 1157 (1956).

[18] R. W. Meier, P. Scherrer, and G. Trumpy, Helv. Phys. Acta 27, 577 (1954); R. Budde and P. Huber, Helv. Phys. Acta 28, 49 (1955); B. M. McCormac, M. F. Steuer, C. D. Bond, and F. L. Hereford, Phys. Rev. 104, 718 (1956); 108, 116 (1957). I. I. Levintov, A. V. Miller, E. Z. Tarumov, and V. N. Shamshev, Nuclear Phys. 3, 237 (1957).

the polarization of elastically scattered protons from carbon had shown that, whereas at high energies such polarizations were quite marked, the effect decreased with decreasing energy until it essentially disappeared at ~50 Mev.[19]

It was to resolve the apparent contradiction above outlined that the present series of experiments[20] were initiated. It was soon apparent from these experiments, as well as from other investigations on the polarization produced in the elastic scattering of both protons[21] and, to a lesser extent, neutrons,[22] that the spin-orbit interaction is indeed very strong at energies below 50 Mev, although a minimum undoubtedly exists in this energy region.

The necessity for a spin-orbit term in the optical model thus was directly confirmed but its addition to the central potential was not without sacrifice, since it permitted even more leeway in fitting of data and the results from the scattering of unpolarized protons proved to be inherently inadequate to fix all of the parameters of the potential. Part of the difficulty arises from the similarity of effects of the real part of the potential and the interaction radius on the one hand and the imaginary part of the potential and the diffuseness parameter on the other.

In the light of the above developments, our experimental objectives were modified to include an attempt to resolve some of the parameter ambiguities. We now elected to proceed by making a broad survey of the angular dependence of the polarization for ~10-Mev protons elastically scattered from a large number of elements. Since, in any case, the optical model must average over the details of nuclear structure, it was felt more worthwhile, initially, to establish general trends over a wide mass range than to obtain high-precision data on a few elements. The present paper gives results on 33 elements.

II. EXPERIMENTAL METHOD

1. General Considerations

It is well known that the differential cross section for the emission of particles in a reaction induced by unpolarized particles is always symmetrical about the axis of incidence. If, however, the incident beam is composed of polarized particles of spin $\frac{1}{2}$ and there is spin-orbit coupling, an azimuthal asymmetry is produced in the angular dependence of the differential cross section. The present investigations are based on the measurement of this azimuthal asymmetry.

In the present discussion polarization always refers to spin expectation values and is defined as follows: An unpolarized beam is assumed to be composed of an equal mixture of two completely but oppositely polarized beams. A partially polarized beam can then be described as a mixture containing a fraction $|P|$ of a completely polarized beam and a fraction $(1-|P|)$ of an unpolarized beam. It follows that the degree of polarization is uniquely defined by the quotient of the difference and sum of the number of particles with spins directed up and down, i.e.,

$$P = (N\uparrow - N\downarrow)/(N\uparrow + N\downarrow). \tag{3}$$

The theory of the polarization process has been treated by a number of authors.[23] Here we invoke the results and terminology as given by Wolfenstein[23] for spin $\frac{1}{2}$ particles.

If the outgoing particles in a nuclear process are polarized, the polarization is described in terms of a polarization vector $\mathbf{P}_1 = \mathbf{n}_1 P_1$ and the angular dependence of this polarization is given by

$$\mathbf{P}_1(\theta_1) = \frac{\mathbf{n}_1}{\sigma(\theta_1)} \sum_{n=0}^{2L_{\max}-1} a_n \cos^n\theta_1 \sin\theta_1, \tag{4}$$

where the symbols have the following meanings: P_1 is the degree of polarization as defined by Eq. (3); $\mathbf{n}_1$ is a unit vector in the direction of the polarization and is defined by $\mathbf{n}_1 \sin\theta_1 = \mathbf{k}_0 \times \mathbf{k}_1$, where $\mathbf{k}_0$ and $\mathbf{k}_1$ are unit vectors in the direction of motion of the incoming and outgoing particles, respectively; θ_1 is the angle between the momentum vectors of the ingoing and outgoing particles; and $\sigma(\theta_1)$ represents the differential cross section for scattering unpolarized particles in the center-of-mass system. The coefficients a_n are dependent upon the particular process involved and $L_{\max}$ is the maximum orbital angular momentum associated with the process.

It is apparent from Eq. (4) that the direction of the polarization is always perpendicular to the plane of the scattering process and that p waves, at least, must contribute to the process for the particles to be polarized. In the event that the particles are polarized, this fact will be revealed by a second scattering for which

[19] A. E. Taylor, *Reports on Progress in Physics* (The Physical Society, London, 1957), Vol. XX, p. 86.

[20] Part of these data has been published previously. See L. Rosen and J. E. Brolley, Jr., *Proceedings of the Second United Nations International Conference on the Peaceful Uses of Atomic Energy, Geneva, 1958* (United Nations, Geneva, 1958), Vol. 14, p. 116.

[21] K. W. Brockman, Jr., Phys. Rev. **110**, 163 (1958); W. A. Blanpied, Phys. Rev. **113**, 1099 (1959); R. E. Warner and W. P. Alford, Phys. Rev. **114**, 1338 (1959); A. B. Robbins and G. W. Greenlees, Phys. Rev. **118**, 803 (1960).

[22] J. D. Clement, F. Boreli, S. D. Darden, W. Haeberli, and H. R. Striebel, Nuclear Phys. **6**, 177 (1958); P. V. Sorokin, A. K. Val'ter, B. V. Gavrilovskii, K. V. Karadzhev, V. I. Man'ko, and A. IA. Taranov, J. Exptl. Theoret. Phys. U.S.S.R. **33**, 606 (1957) [translation: Soviet Phys.—JETP **6**, 466 (1958)].

[23] L. Wolfenstein, Phys. Rev. **75**, 1664 (1949); *Annual Review of Nuclear Science* (Annual Reviews, Inc., Palo Alto, 1956), Vol. 6, p. 43. J. V. Lepore, Phys. Rev. **79**, 137 (1950); R. J. Blin-Stoyle, Proc. Phys. Soc. (London) **A65**, 949 (1952); A. Simon and T. A. Welton, Phys. Rev. **90**, 1036 (1953); A. Simon, Phys. Rev. **92**, 1050 (1953). G. Breit and J. S. McIntosh, *Handbuch der Physik* (Springer-Verlag, Berlin, 1959), Vol. XLI/1, p. 466.
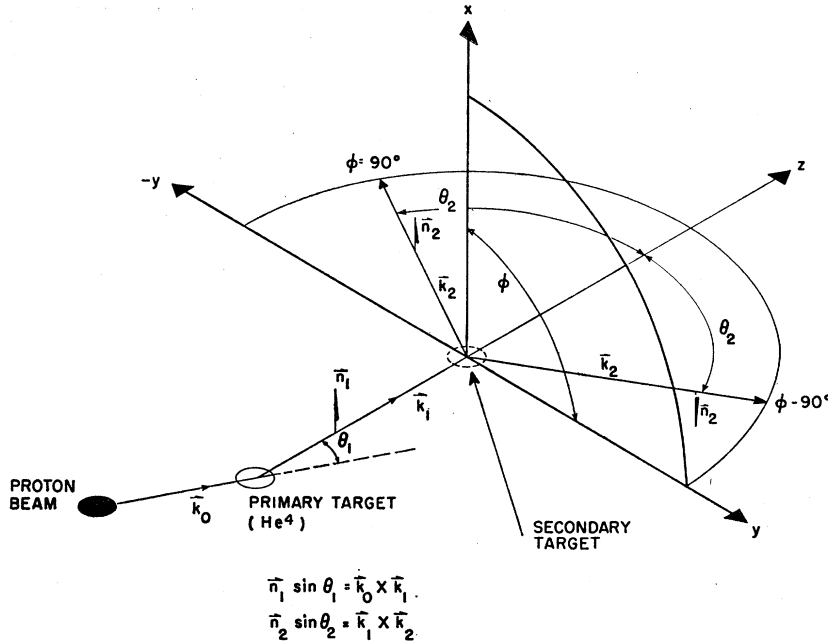
FIG. 1. The double-scattering geometry.

$$\bar{n}_1 \sin\theta_1 = \bar{k}_0 \times \bar{k}_1 .$$

$$\bar{n}_2 \sin\theta_2 = \bar{k}_1 \times \bar{k}_2 .$$

the differential cross section is given by

$$\sigma(\theta_2,\phi) = \sigma(\theta_2)_{\mathrm{un}} + \mathbf{n}_2 \cdot \mathbf{P}_1 \sum_{n=0}^{2L_{\mathrm{max}}-1} b_n \cos^n\theta_2 \sin\theta_2, \quad (5)$$

where $\sigma(\theta_2)_{\mathrm{un}}$ is the differential cross section for scattering unpolarized particles through angle θ_2 and $\mathbf{n}_2$ is a unit vector perpendicular to the plane of the second scattering process. θ and ϕ are the usual spherical polar coordinates measured from the z axis (direction of incidence) and x axis, respectively.

If now the direction of polarization is taken along the x axis (Fig. 1), and, if furthermore, only first and second scatterings are considered which take place in the y-z plane ($\mathbf{n}_2 \cdot \mathbf{n}_1 = \sin\phi = \pm 1$), then Eq. (5) can be written

$$\sigma[\theta_2, (\phi = \pm 90°)]$$

$$= \sigma(\theta_2)_{\mathrm{un}} \pm P_1 \sum_{n=0}^{2L_{\mathrm{max}}-1} b_n \cos^n\theta_2 \sin\theta_2. \quad (6)$$

In analogy with Eq. (4), the summation in Eq. (6) may be replaced by the product of $\sigma(\theta_2)$ and P_2 (the polarization that would be produced by scattering an unpolarized beam through θ_2). Therefore, in a coplanar double-scattering process the left-right ratio is given by

$$R = \frac{\sigma_l(\theta_2)}{\sigma_r(\theta_2)} = \frac{1 + P_1 P_2}{1 - P_1 P_2}. \quad (7)$$

It follows from Eq. (7) that the fractional difference in intensity, A, for those nucleons scattered twice to the left or right as compared to those scattered once

to the left and once to the right is given by

$$A = \frac{\sigma_l(\theta_2) - \sigma_r(\theta_2)}{\sigma_l(\theta_2) + \sigma_r(\theta_2)} = \frac{R-1}{R+1} = P_1 P_2. \quad (8)$$

The possibility of producing polarized nucleons by elastic scattering was first recognized by Schwinger.[24] He suggested that fast nucleons might be polarized by scattering from He^4 since Li^5 was thought to contain a low-lying resonance level which is split by spin-orbit coupling (the last proton in Li^5 is presumed to be coupled to He^4 either in a $P_{1/2}$ or $P_{3/2}$ state, depending upon the excitation of the Li^5). A phase-shift analysis, by Critchfield and Dodder,[25] of the Minnesota p-He^4 elastic scattering data showed that only $S_{1/2}$, $P_{1/2}$, and $P_{3/2}$ partial waves enter into the interactions. They suggested that the ordering of the $P_{1/2}$ and $P_{3/2}$ levels could be ascertained by measuring the sign of the polarization of the scattered protons. Heusinkveld and Freier[26] carried out the indicated experiments which simultaneously demonstrated that the $P_{1/2}$ level is the higher and that polarized nucleons can indeed be generated in the way originally proposed by Schwinger. A number of additional experiments[27] have now established the energy dependence of the polarization from p-He^4 scattering up to 17 Mev.

[24] J. Schwinger, Phys. Rev. 69, 681 (1946); Phys. Rev. 73, 407 (1948).
[25] C. L. Critchfield and D. C. Dodder, Phys. Rev. 76, 602 (1949).
[26] M. Heusinkveld and G. Freier, Phys. Rev. 85, 80 (1952).
[27] M. J. Scott and R. E. Segel, Phys. Rev. 100, 1244 (1955); A. E. Juveland and W. Jentschke, Z. Physik 144, 521 (1956); K. W. Brockman, Jr., Phys. Rev. 102, 391 (1956); L. Rosen and J. E. Brolley, Jr., Phys. Rev. 107, 1454 (1957); M. J. Scott, Phys. Rev. 110, 1398 (1958).

2. Instrumentation

In the present experiments p-He^4 scattering is used to produce a beam of essentially fully polarized 10-Mev protons of intensity $\sim 10^{10}$ steradian^{-1} sec^{-1}. The technique employed is rather the inverse of what had been done heretofore. The polarized beam is achieved by irradiating a gaseous hydrogen target with 25-Mev alpha particles and extracting the protons which are deflected through 130° in the c.m. system, i.e., those protons which recoil at 25° to the primary beam direction. This procedure has the advantage of providing completely polarized protons in a convenient direction and of an energy in excess of 10 Mev, whereas the scattering takes place with the higher cross section appropriate to protons of approximately half that energy. Furthermore the solid angle transformation is very favorable from the intensity standpoint. The experimental arrangement is schematically illustrated in Fig. 2. Alpha particles are accelerated by the Los Alamos variable-energy cyclotron. An ion-optical system composed of vertical and horizontal steering magnets, strong-focussing magnets and 30° turning magnet conducts 5–10 μa of the deflected beam through 4 ft of 0.5-in. i.d. iron collimators which are placed in the shield wall separating the cyclotron vault from the experimental room. The α beam is defined by six $\frac{3}{8}$-in. diameter circular gold diaphragms installed at 8-in. intervals along the collimation channel. The $\frac{3}{8}$-in. diameter beam enters the hydrogen target through a 0.5-in. circular aperture which is sealed by a 0.0005-in. molybdenum "window." The hydrogen target is pressurized to 4 atmospheres and is sufficiently long to absorb all the energy of the α beam, thus avoiding reactions which could give rise to neutrons or gamma rays. The H$_2$

target also serves as a Faraday cup and is connected to a current integrator for purposes of monitoring the primary beam.

The polarized protons enter the second scattering chamber through a series of rectangular apertures $\frac{1}{8}$ in. wide (in a plane of scattering) by $\frac{1}{4}$ in. high which define the polarized beam direction to $\pm 2°$. The H$_2$ is excluded from the second chamber by a 0.0005-in. aluminum "window." The twice-scattered protons are then detected in Ilford $C2$ emulsions placed in the second scattering chamber as illustrated in Fig. 2. Rectangular collimation holes allow a judicious compromise between intensity and angular resolution by taking advantage of the slowly varying azimuthal dependence of the polarization near $\phi = \pm 90°$ [see Eq. (5)].

The polarimeter is designed to eliminate the necessity for manual alignment provided the various components are machined to tolerance and assembled with care. Spring clamps hold the detectors against two flat surfaces symmetrically situated with respect to the plane of symmetry through the collimator apertures and perpendicular to the scattering plane. When the second scatterer is a gas, the reaction volume is defined by two concentric hollow cylinders, one of which is "telescopic" so that the spacing between the cylinder faces can be adjusted to give the angular resolution desired. Only those protons scattered from the reaction volume which can be seen by a given point on the detectors can reach that point directly. Each position along the detectors thus defines a mean scattering angle. An important feature of this arrangement is that data may be taken at many angles simultaneously, although the mean energy of the polarized protons is slightly
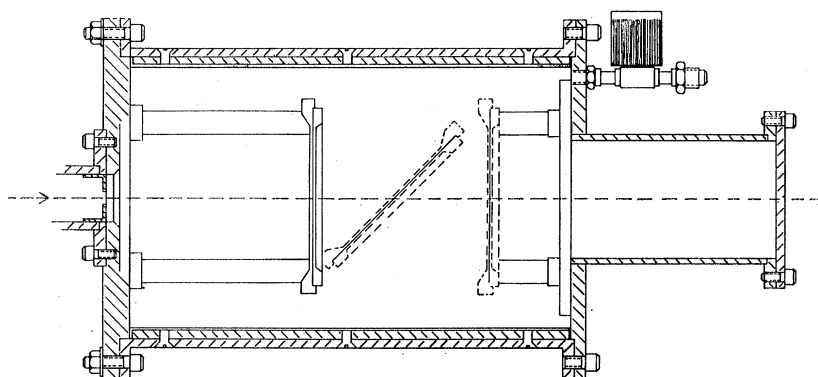

FIG. 2. Experimental arrangement.
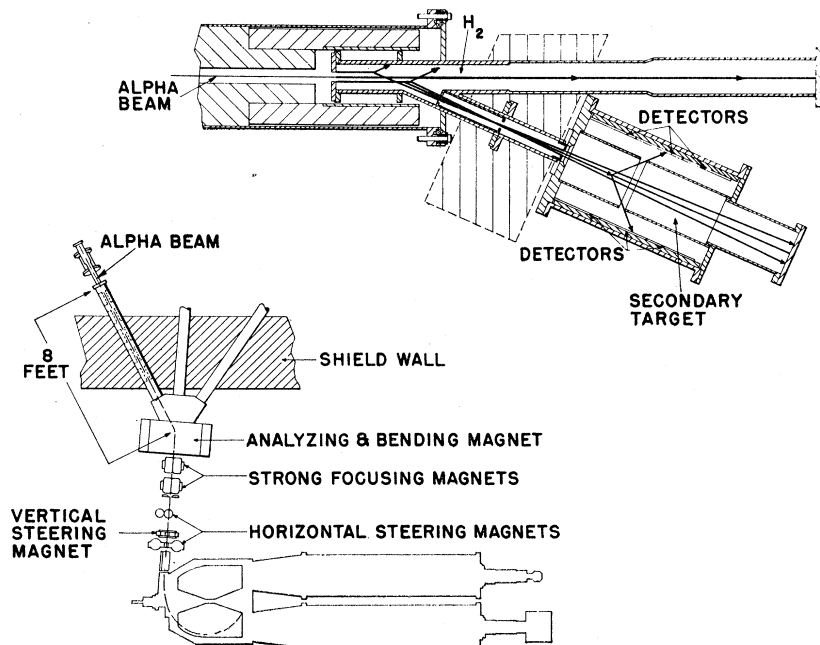
Fig. 3. Second-scattering chamber for solid targets.

different from angle to angle. The scattering geometry for solid targets is illustrated in Fig. 3. Although the mean energy is the same at every angle, three runs must be made in order to cover the entire angular interval.

3. Tests of Apparatus

Checks were made to ascertain whether the apparatus was built to the specified precision, the crucial point being the detection of instrumental asymmetries which will give rise to a value of R different from unity.

One of these tests consisted of measuring the proton beam intensity profile by counting tracks in emulsions placed at the entrance to the second scattering chamber and adjacent to the final slit of the proton collimation system, and also at 20 cm downstream. The density distributions obtained proved to be symmetrical with respect to the median plane to well within acceptable limits. In addition, the intensities and the energy spread in the beam were very close to the calculated values based on p-α cross-section data. It will be noticed that there is a measure of compensation with regard to both energy spread and intensity in the second-scattering volume. The protons which recoil at the largest angles from the lowest energy alphas (those alphas traveling farthest in the H_2 target) traverse the shortest path in H_2 while the inverse situation obtains for the protons which start off with the highest energy. A second check consisted of scattering the polarized proton beam from a gold target. It is known that the scattering of 10-Mev protons by gold is sufficiently Coulombic that no left-right asymmetry should be observed. The values of R, Eq. (7), obtained from the gold experiments varied between 0.98 and 1.02 as was to be expected from statistical uncertainties alone.

4. Plate Analysis

The nuclear emulsions were generally of sufficient thickness to stop the highest energy protons reaching them. The plates were scanned in swaths transverse to the horizontal projection of the tracks. A track was accepted for measurement if it started in the emulsion

surface, its direction intersected the reaction volume viewed by the plate area being scanned, and its grain density did not decrease with increasing distance from the emulsion surface. Measurements were made of the horizontal projection and total dip of each track from which it was possible to deduce the range and hence the energy of each proton which entered the emulsion. In each exposure the mean energy in the second scattering volume was determined from the ranges of the scattered protons after making corrections for the loss of energy in the collisions and in the material between the center of the scattering volume and the area of the detector which viewed that volume. Great care was taken to scan corresponding areas of each set of plates from a given run. By using a microscope to delineate the bounds of each area scanned, it was possible to insure that corresponding areas represented the same mean scattering angle to within a few tenths of 1°.

5. Background

In the initial experiments, complete range and angular distributions were obtained for all the tracks recorded in the detectors. The results showed that the greatest portion of the tracks did indeed come from the direction of the appropriate scattering volume and that background tracks would be no problem at all in the forward hemisphere and only a minor nuisance in the backward hemisphere. Most of the background tracks were due to neutron-produced proton recoils, and those which appeared to start in the emulsion surface at the proper angle were usually either too short to be ascribed to elastic scattering or their grain densities changed in the wrong direction. Gamma-ray background, although limiting the duration of the runs, does not produce tracks which can be confused with those due to protons.

The above conclusions were verified by background runs made without the second scatterer. Only in a few cases, where cross sections for elastic scattering of protons through large angles are unusually small, was it necessary to use the results of our background runs to correct the data, and even then the corrections to R did not exceed 10%.

6. Treatment of Data

For every plate area-analyzed, the measurements on each track were plotted on a coordinate system in which the ordinate is proportional to the horizontal projected length (as seen in the microscope) and the abscissa to the dip (projected length along the direction perpendicular to the plane of the emulsion.) This plot was used to separate the elastic from the inelastic scattering events. In difficult cases the absolute range of each track was determined and a range distribution plotted. In either case the data were analyzed to yield the number of elastically scattered protons in corresponding areas of each pair of detectors. From the number of tracks scattered to the left and to the right was calculated the scattering asymmetry, A, according to Eq. (8). The polarization which would be produced by the elastic scattering of unpolarized protons by the second target is then given by[28] $P_2 = A/\bar{P}_1$, where $\bar{P}_1$ is the average value of the polarization of protons scattered by 25-Mev He^4 nuclei at $25 \pm 1°$. $\bar{P}_1$ was calculated by numerically integrating the equation,

$$\bar{P}_1 = \int P_1(\theta_1)\sigma(\theta_1)d\omega_1 \Big/ \int \sigma(\theta_1)d\omega_1, \qquad (9)$$

and found to be 0.96 for our geometry. The values of $P_1(\theta_1)$ were taken from calculations based on the phase shifts for p-He^4 scattering[29] which yield the same polarizations as are obtained directly from polarization measurements involving the double scattering[30] of protons by He^4.

Our sign convention is the same as that of Wolfenstein[23] who takes the polarization to be positive[31] if the nucleon spin is in the direction $k_0 \times k_1$ (Fig. 1). The sign of the polarization in p-He^4 scattering, as deduced from the phase shifts, is used to establish the spin direction of our polarized beam.

All but two of the targets used were either spectroscopically pure gases or solids of natural isotopic abundance and the P_2 values obtained apply to the appropriate isotopic mixture. One of the two exceptions was the boron target for which separated B^{10} was used. The other exception was fluorine which could not be used in its pure state due to its corrosive nature. Therefore A values were measured for CF_4 and C in two separate experiments and the polarization produced by the fluorine was calculated from

$$P_F = \left[\frac{A_{CF_4}}{P_1}\left(1 + 4\frac{\sigma_F}{\sigma_C}\right) - P_C\right] \Big/ \left(4\frac{\sigma_F}{\sigma_C}\right). \qquad (10)$$

[28] L. Rosen and J. E. Brolley, Jr., Phys. Rev. Letters **2**, 98 (1959). The polarization-asymmetry equality ($P_2 = A$ when $P_1 = 1$) is based on time-reversal invariance and has been verified by experiment at these energies.

[29] J. L. Gammel and R. M. Thaler (private communication).

[30] L. Rosen and J. E. Brolley, Jr., Phys. Rev. **107**, 1454 (1957).

[31] This convention is the same as that adopted at the 1960 Polarization Conference at Basel, Switzerland, Helv. Phys. Acta (to be published).

In addition to the polarization at each scattering angle, the relative cross sections for elastically scattered unpolarized protons were also obtained by simply averaging the yields for scattering to the left and to the right [Eq. (6)].

7. Second Order Geometry Effects

The quantity actually measured in these experiments is the product of P_2 and $\langle\cos(\Delta\phi)\rangle_{av}$. Since the collimator slits and swath length confined $\Delta\phi$ to $\pm 11°$, $\cos(\Delta\phi)$ averaged over the permitted angular range is ~ 0.995.

Although the polarimeter was designed to minimize second order geometry effects which give rise to left-right asymmetries, these were not entirely excluded. It was established by both calculation and experiment that such asymmetries were essentially absent for the gas targets and for solid targets in the plane perpendicular to the proton collimation slit axis. However, in order to obtain data on solid targets in the angular region between 80° and 100°, it was necessary to tilt the target as indicated in Fig. 3 and this gives rise to an instrumental asymmetry. The anomalous polarization produced by this asymmetry is $P_0 = (R_0 - 1)/(R_0 + 1)$, where R_0 is the instrumental left-right asymmetry. R_0 was calculated by numerical integration over the two scattering volumes and the plate area analyzed and found to vary between 0.94 and 1.05. It was necessary to perform this calculation for each target element used in the solid state because R_0 is sensitive to the differential cross sections for elastic scattering. Having obtained P_0, the observed value of P was divided by $(1 + P_0)$ or $(1 - P_0)$, depending upon whether P_0 and P were of like or opposite sign.

8. Errors

From Eq. (6), the rms random error in the measured polarization is given by

$$(\Delta P_2)_{rms} = \left\{\left[\frac{2(\Delta R)_{rms}}{P_1(R+1)^2}\right]^2 + \left[\frac{P_2(\Delta P_1)_{rms}}{P_1}\right]^2\right\}^{\frac{1}{2}}. \qquad (11)$$

Since the uncertainty in P_1 is less than 0.01, the second term is quite negligible. The dominant contribution to ΔP_2 resides in the statistical uncertainty of R. Although the goal was to analyze ~ 400 tracks for each set of areas at a given angle, this could not always be achieved without an excessive sacrifice in angular resolution.

The major systematic error was introduced by the ever-present possibility of unresolved inelastic scattering corresponding to low-lying levels in the residual nucleus. Levels removed from the ground state by less than 1.5 Mev were, in general, not resolvable. The error in the measured polarization resulting from the inclusion, in the elastic scattering peak, of inelastically scattered protons is given by

$$\Delta P = P_2 - P_e = \frac{-\sigma_i}{\sigma_e + \sigma_i}(P_e - P_i), \qquad (12)$$

where P_e and P_i are, respectively, the polarization due to elastic scattering and the polarization due to the unresolved inelastic scattering. σ_e and σ_i refer to the corresponding cross sections for unpolarized protons. The average value of ΔP is approximately that for which P_i is zero, an assignment which is rigorously correct if a true compound nucleus is formed. In order to estimate σ_i we have compared our relative elastic scattering cross sections, obtained as previously described, with equivalent cross sections obtained from single-scattering experiments (such as the experiments of Hintz[4] at 10 Mev under conditions permitting much better energy resolution). On the basis of the σ_i values so obtained we conclude that ΔP is less than 0.02 for angles smaller than 90°. At back angles, however, ΔP could be as large as 0.05.

The remaining systematic uncertainties are of little consequence. The most important is the one associated with P_0 which applies only to solid targets in the angular region 80°–100° and is certainly less than 0.015. The error in P_2 associated with the plate area scanned and with the position of that area is ~0.01. The depolari-

TABLE I. Angular dependence of the polarization of protons elastically scattered by various elements. The mean energy of the incident proton is listed in parenthesis.

D (~10 Mev)		He (~10 Mev)		Be (11.4 Mev)		B10 (~10 Mev)		C (11.7 Mev)		N (10.4 Mev)	
θ (deg)	P_2 (%)	θ (deg)	P_2 (%)	θ (deg)	P_2 (%)	θ (deg)	P_2 (%)	θ (deg)	P_2 (%)	θ (deg)	P_2 (%)
38.5	+5±10	33	−22± 4	35	−10± 4	31	−20± 5	33.5	−19± 5	29	−28± 5
41.5	+2± 5	38.5	−32± 4	46.5	−21± 4	33	−25± 5	38	−28± 4	30.5	−36± 5
51.5	−9±11	56.5	−51± 5	58.5	−35± 5	43.5	−26± 5	44.5	−50± 5	36.5	−45± 5
55.5	+5± 6	72.5	−67± 4	67	−51± 5	56.5	−41± 5	48	−59± 5	39.5	−45± 6
59.5	0±13	82.5	−82± 7	71.5	−46± 6	65	−35± 5	56	−77± 5	40.5	−56± 5
65.5	+3± 5	94.5	−80± 2	75.5	−26± 5	75.5	+6± 6	60	−87± 5	45	−64± 4
75	0± 5	113.5	+4± 6	89	+19± 6	88	+6± 8	64.5	−82± 5	47	−60± 5
76	−8± 4	133.5	$+99^{+1}_{-2}$	97.5	+21± 7	96	+3± 8	69.5	+7± 9	52.5	−72± 5
90	+5± 7	146.5	+81± 4	107	+11± 6			73.5	+60± 7	60	−76± 5
93	+2± 9			116.5	+2± 7			86.5	+55± 5	66	−50± 7
94	−6±10	151.5	+59± 8	128	−4± 6			95	+30± 6	70.5	+4± 9
98	−4±16			144	+2± 9			104.5	+15± 6	78.5	+40± 6
99	−2±12							115.5	−8± 6	87.5	+40± 5
104	+8± 9							126.5	−26± 7	94.5	+21± 7
105	−5± 9							132.5	−35± 8	101.5	−4± 7
109.5	−6± 9							142	−47± 8	112.5	−64± 6
110	−5± 7									120	−63±15
120	−2±13									130.5	−38± 8
123.5	−2±10									140.5	−20±10
124	−16±10										
128	+1± 9										

TABLE II. Angular dependence of the polarization of protons elastically scattered by various elements. The mean energy of the incident proton is listed in parenthesis.

O (~10 Mev)		F (10.2 Mev)		Ne (10.3 Mev)		Mg (10.7 Mev)		Al (10.2 Mev)		S (10.4 Mev)	
θ (deg)	P_2 (%)	θ (deg)	P_2 (%)	θ (deg)	P_2 (%)	θ (deg)	P_2 (%)	θ (deg)	P_2 (%)	θ (deg)	P_2 (%)
35.5	−31± 5	27	−13± 6	27.5	−18± 5	32	−16± 6	32	−1± 5	31	0± 5
41	−47± 5	32.5	−2± 5	37	−20± 5	43	−2± 6	43	−8± 5	41	+17± 5
47	−37± 7	43	+3± 7	38.5	−20± 6	54.5	+32± 8	48	+14± 5	53.5	+45± 5
49	−53± 6	48	+6±11	44	−19± 7	56.5	+30± 9	54	+22± 5	61.5	+30± 5
54.5	−57± 9	52	+19±11	48	−9± 8	63.5	+30± 7	63.5	+2± 5	71.5	+8± 6
62.5	−38±13	56.5	+31±11	49.5	−9±12	74	−20± 8	74	−10± 6	84	−49± 5
71.5	+44±10	62	+28±10	59	+52± 8	84.5	−30± 7	84	−30± 5	92	−66± 7
75.5	+24±13	71	0± 7	69	+19± 7	92.5	−41±11	93	−40± 7	102	−42± 9
78	+23± 7	80.5	−1± 7	78.5	−6± 6	102.5	−55±12	102	−54± 8	111.5	+43±11
83	+16± 6	88.5	−28± 7	89.5	−13± 5	112	−8± 9	112	0± 8	118.5	+29±12
91	−27± 7	98.5	−36± 9	98.5	−27± 7	118	+42±11	118	+28± 8	123.5	+23±12
100	−48± 6	108.5	−56± 9	108.5	−47± 8	131	+29±12	130.5	+34± 9	131.5	+16±11
113	−72± 6	118	−51±11	120.5	−64± 9	140.5	+5±11	140.5	+56± 9		
123	−71± 7	130	−1±11	126	−58± 9	150.5	−33±12				
132.5	−70± 7			130.5	−40±10						
134	−80± 8			140.5	+16± 9						
145.5	−14±13										
150.5	+4±15										

TABLE III. Angular dependence of the polarization of protons elastically scattered by various elements. The mean energy of the incident proton is listed in parenthesis.

A (9.8 Mev)		Ca (10.7 Mev)		Ti (10.4 Mev)		V (10.2 Mev)		Mn (10.3 Mev)		Fe (10.1 Mev)	
θ (deg)	P_2 (%)	θ (deg)	P_2 (%)	θ (deg)	P_2 (%)	θ (deg)	P_2 (%)	θ (deg)	P_2 (%)	θ (deg)	P_2 (%)
26.5	−3± 4	30.5	−2± 5	31.5	−8± 5	30.5	+7± 4	30.5	+2± 5	31.5	+4± 5
31.5	+2± 5	41	+18± 5	42.5	+1± 5	40.5	+4± 5	40.5	−9± 5	42	0± 5
42.5	+3± 4	53	+12± 5	53.5	0± 5	53	−11± 5	53	−5± 5	53.5	−3± 4
52.5	−4± 5	61.5	+11± 5	62.5	−24± 5	61	−16± 6	61	−20± 5	62.5	−5± 5
63.5	−29± 5	71.5	−14± 5	70	−42± 5	71	−12± 6	71	−23± 7	73	−20± 5
69	−33± 6	83.5	−32± 8	83	−13± 6	83	+40± 8	83	+15± 8	83	+19± 6
72.5	−46± 7	91.5	+11± 9	91	+44± 7	91	+43± 8	91	+30± 8	91	+34± 7
81.5	−36± 9	101.5	+60± 7	101	+38± 7	101	+42± 8	101	+20± 8	101	+23± 7
90.5	+5±12	111.5	+58± 7	111	+21± 7	111	+1± 8	111	+3± 9	111	+5± 8
100	+66±13	117	+43± 9	117	+7± 7	118	−4± 9	117.5	−11±13	117	+7± 9
106.5	+45±13	123.5	+17± 9	130	−18±10	123	−18±10	123	−26±10	130	−18±13
120	−18± 9			140	−50±12	131	−40±13	131	−16±14		
128.5	−6± 9			150	+14±15	140.5	−45±19				

TABLE IV. Angular dependence of the polarization of protons elastically scattered by various elements. The mean energy of the incident proton is listed in parenthesis.

Co (10.0 Mev)		Ni (10.0 Mev)		Cu (~10 Mev)		Zn (10.5 Mev)		Kr (9.9 Mev)		Zr (10.5 Mev)	
θ (deg)	P_2 (%)	θ (deg)	P_2 (%)	θ (deg)	P_2 (%)	θ (deg)	P_2 (%)	θ (deg)	P_2 (%)	θ (deg)	P_2 (%)
30.5	+3± 4	31.5	0± 4	29.5	−2± 4	31.5	+9± 5			31.5	−1± 5
40.5	+6± 5	42	−3± 4	35	+1± 4	42.5	−10± 5	25	+2± 4	42	−2± 5
53	−18± 5	53.5	−15± 5	40	−3± 4	56	−20± 5	31	−4± 4	49	−8± 5
61	−18± 5	62.5	−22± 5	44	−6± 4	61.5	−17± 6	36.5	−1± 5	53	−5± 5
71	−5± 8	73	−20± 5	48.5	−10± 4	70	+4± 6	41.5	−4± 5	61	+3± 5
83	+37± 7	83	+13± 5	52.5	−16± 4	75	+30± 7	46	−2± 5	69.5	+18± 5
91	+32± 9	91	+24± 7	55.5	−20± 4	83	+21± 5	55	0± 5	82.5	+2± 6
101	+20± 9	101	+16± 7	58.5	−17± 4	91	+20± 7	64.5	+1± 6	90.5	−11± 7
111	+4±10	111	−3± 6	61.5	−17± 4	101	−4± 9	73.5	+3± 5	100.5	−15± 7
118	−15±12	117	−9± 7	66.5	−10± 4	112	−14±10	81.5	+2± 6	111.5	−12± 8
123	−9±13	130	−23±12	70	+1± 5	117	−29± 9	91.5	−6± 7	122.5	+7±11
131	+6±18			76.5	+20± 7	123.5	−30±14	100.5	−1±11	129.5	+20±11
				87	+13± 7	129.5	−33±16	113.5	−14±17		
				97	+7± 8	139.5	+13±26	128	+16±18		
				101	−2± 8	150	+23±24				
				117.5	−11± 6						
				122.5	−15± 7						
				124	−6± 9						
				126.5	−12± 8						
				129	−10± 8						
				132	+3± 9						
				134	+3±11						

zation effect of the hydrogen and aluminum window traversed by the polarized beam is negligible.

III. RESULTS

The polarization results deduced from the present experiments are presented in Tables I to VI. The element studied is denoted in the top row, followed, in parenthesis, by the mean energy of the polarized proton beam. In the two columns under each element are listed, from left to right, the scattering angle in the c.m. coordinate system and the polarization which is produced when an unpolarized proton beam of the appropriate energy is scattered by the indicated element at the specified angle. The polarization listed is numerically equal to P_2 of Eq. (8) and is calculated as described in the text. The tabulated uncertainties represent a quadratic combination of the various errors described in the previous section. These data were not corrected for and the indicated uncertainties do not take account of the distortions produced by finite angular resolution.

Figures 4 and 5 display the angular dependence of the polarization for all elements studied, together with the angular dependence of the elastic scattering from precise single-scattering experiments near 10 Mev. The scale on the right refers to the polarization while the scale on the left denotes the ratio of elastic to Coulomb scattering. Relative elastic scattering data from the present experiments (normalized to $\sigma/\sigma_R = 1$ at the

TABLE V. Angular dependence of the polarization of protons elastically scattered by various elements.
The mean energy of the incident proton is listed in parenthesis.

Nb (10.5 Mev)		Mo (10.4 Mev)		Rh (11.2 Mev)		Pd (10.8 Mev)		Ag (10.6 Mev)		Cd (10.9 Mev)	
θ (deg)	P_2 (%)	θ (deg)	P_2 (%)	θ (deg)	P_2 (%)	θ (deg)	P_2 (%)	θ (deg)	P_2 (%)	θ (deg)	P_2 (%)
31.5	−9± 5	31.5	−11± 5	31.5	−13± 5	31.5	−10± 4	31.5	+3± 5	31.5	+1± 6
40.5	−2± 4	42	−8± 5	42	−5± 5	42	+5± 5	42	−5± 5	42	0± 5
52.5	−5± 5	49	−9± 4	53	−9± 5	46	−7± 4	53	−4± 4	53	−2± 5
60.5	+3± 5	53	+1± 4	61	+5± 5	53	+4± 5	62	+7± 5	61	−1± 5
70.5	+13± 5	61	0± 5	69.5	+7± 5	61	0± 4	72.5	+8± 5	69.5	+5± 5
82.5	−3± 5	69.5	+2± 5	82.5	−6± 6	69.5	+7± 4	82.5	−11± 5	82.5	−5± 6
90.5	−9± 7	82.5	−5± 5	90.5	−14± 8	82.5	−11± 6	90.5	−7± 7	90.5	−7± 8
100.5	−27± 7	90.5	−4± 7	100.5	−21± 8	90.5	−18± 8	100.5	−9± 7	100.5	−3± 9
110.5	−24± 8	97	−12± 7	110.5	−3±10	100.5	−9± 7	111.5	+8± 8	111.5	+14±11
117.5	−9±18	100.5	−18± 8	122.5	−26±11	110.5	−4± 9	116.5	+3± 9	122.5	+18±12
122.5	+14±12	110.5	−6± 9	129.5	0±15	117.5	−23±10	129.5	+2±12	129.5	−29±14
130.5	+35±14	116.5	+5± 9			129.5	−11±11				
140.5	+43±15	122.5	−2±11								
		129.5	+19±10								

smallest angle) are shown for the elements which have not been studied in single scattering experiments. The letters in parenthesis on each figure reference the elastic scattering data. The vertical bars on the polarization points indicate the statistical errors only, whereas the horizontal bars indicate the angular definition (total angle of acceptance of scattered protons). The elastic scattering cross section values obtained from the present experiments are all relative and they contain several large uncertainties not present in the polarization data. In the evaluation of the polarization it was only necessary to ensure that corresponding plate areas subtended the same solid angle at the scattering volume. However, calculation of the elastic cross section required the evaluation of the solid angle at each datum point. In addition it was necessary to normalize the target thicknesses and integrated currents for all the runs involving a given element. As a consequence the relative accuracy of the elastic scattering cross section is ∼20%.

TABLE VI. Angular dependence of the polarization of protons elastically scattered by various elements. The mean energy of the incident proton is listed in parenthesis.

In (10.4 Mev)		Xe (9.2 Mev)		Au (∼10 Mev)	
θ (deg)	P_2 (%)	θ (deg)	P_2 (%)	θ (deg)	P_2 (%)
31	+1± 5	26	+2± 5	41.5	+1± 5
42	−6± 4	31	+5± 5	52.5	−2± 5
53	+3± 4	42	−2± 5	62	+9± 5
61	+5± 5	50	−1± 5	72.5	−4± 5
69.5	+3± 5	57	−1± 5	82.5	+1± 3
82.5	−1± 5	59.5	−11± 5	90.5	+1± 6
90.5	−17± 7	64	−2± 5	100.5	−7± 6
100.5	0± 7	68.5	−2± 5	110.5	−3± 7
111.5	+8± 7	78	−1± 5	116.5	+5± 7
122.5	−2± 9	86	−2± 5	129	−8± 7
129.5	−5±11	95.5	−7± 8	139	+16±13
139.5	−2±14	105.5	−7± 9		
		114.5	−6± 8		
		128	−6± 8		

These data are, however, adequate to establish the positions of the maxima and minima.

IV. DISCUSSION

The smooth curves in Figs. 4 and 5 represent fits to the data using an optical model potential including a spin-orbit term proportional to the derivative of the real part of the central potential. The terms in the potential which describe the purely nuclear interaction can be written

$$V(r) = (V+iW)\rho(r) + \frac{\gamma V}{2}\left(\frac{\hbar}{mc}\right)^2 \frac{1}{r}\frac{d\rho}{dr}\mathbf{l}\cdot\mathbf{s}, \quad (13)$$

where

$$\rho(r) = \left[1+\exp\left(\frac{r-R}{a}\right)\right]^{-1}. \quad (14)$$

For the Coulomb potential we used "Family 2 (b)" of Ford and Hill.[32] In Eqs. (13) and (14), R is the radius at which the potential depth is half its maximum value, a is a constant which determines the diffuseness of the nuclear surface, m represents the proton mass, and $\mathbf{l}$ and $\mathbf{s}$ are the orbital angular momentum and spin, respectively, in units of $\hbar$.

The curves illustrated represent an attempt to fit all of the data with the same values of the five parameters in the above equations. These probably represent the minimal number that can be realistically considered.

For an assumed potential, the calculations consisted of an exact numerical integration of the Schrödinger equation which determines the motion of the proton in the field of the target nucleus. It is then possible to construct the angular dependence of the polarization and elastic scattering. The trial set of parameters was then empirically varied until a reasonable fit was obtained to the data on four elements, Be, Ne, A, and Ni; these elements were chosen in order to span the mass region under investigation. Each calculation was

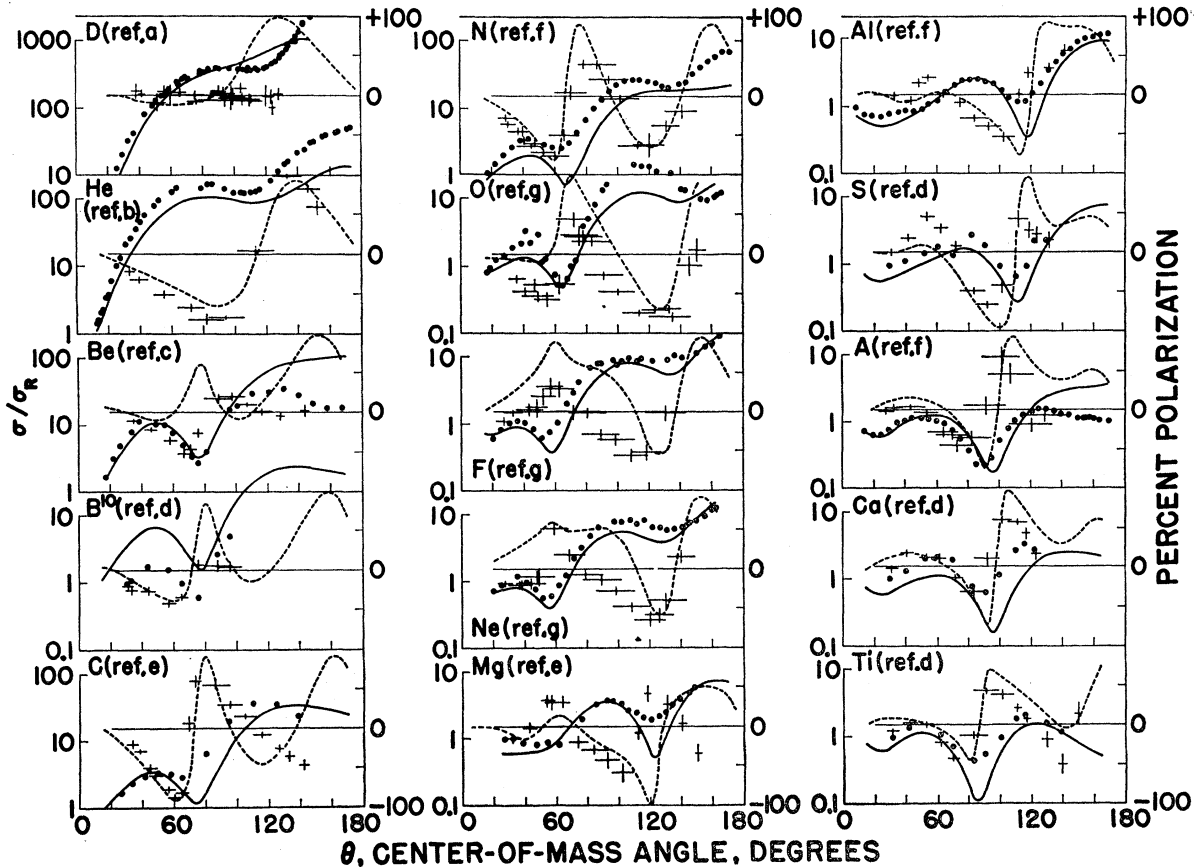[32] D. L. Hill and K. W. Ford, Phys. Rev. 94, 1617 (1954).

FIG. 4. Angular dependence of the polarization (+) and elastic scattering (●) of protons scattered by various elements. The elastic scattering data were reproduced from the following references: (a) J. C. Allred, A. H. Armstrong, R. O. Bondelid, and L. Rosen, Phys. Rev. **88**, 433 (1952). (b) T. M. Putnam, Phys. Rev. **87**, 932 (1952). (c) S. W. Rasmussen, Phys. Rev. **103**, 186 (1956). (d) Relative elastic scattering distribution calculated from yield of polarization data. (e) G. E. Fischer, Phys. Rev. **96**, 704 (1954). (f) N. M. Hintz, Phys. Rev. **106**, 1201 (1957). (g) W. M. Gibson, D. J. Prowse, and J. Rotblat, Proc. Roy. Soc. (London) **A243**, 237 (1957). (h) G. W. Greenlees, L. G. Kuo, and M. Petravić, Proc. Roy. Soc. (London) **A243**, 206 (1957).

made at the energy of the elastic scattering data for that particular element.

The calculations were carried out on an IBM 704. The parameters finally adopted for all the elements are:

$$R = 1.2A^{\frac{1}{3}}\,\text{f}, \quad V = -55\,\text{Mev}, \quad W = -6\,\text{Mev}, \quad \gamma = +23, \quad a = 0.50\,\text{f}.$$

The following remarks will be concerned with the polarization results only. The significance of available elastic scattering data in the energy region under consideration has been adequately discussed in a number of papers already referred to.

Although one might reasonably have expected from an extrapolation of the high-energy work that polarization effects would be quite small at intermediate energies, this has turned out to be not the case. In all complex nuclei for which the Coulomb barrier is less than the incident energy, very large polarizations are the rule. As might be expected, the magnitude of this polarization decreases as the Coulomb barrier increases.

Just as the outstanding gross feature of the elastic scattering data is its diffraction-like character, so is the dominant feature of the polarization data its smooth dependence on scattering angle and target size, with the extremum points decreasing in absolute magnitude and moving to smaller angles as the mass of the target increases. (Fig. 6.) Furthermore there appears to exist a strong correlation between the angular dependence of elastic scattering and of polarization. In particular, the extrema of the elastic scattering curves correspond approximately to zeros in the polarization. In fact the polarization appears to be roughly proportional to the derivative of the elastic scattering angular distribution.[33]

An obvious inference from the above observations is that spin "up" protons see an average potential which differs significantly from that seen by spin "down" protons. It would then be so that the diffraction minima for unpolarized protons (which can be considered as composed of equal numbers of spin "up" and spin

---

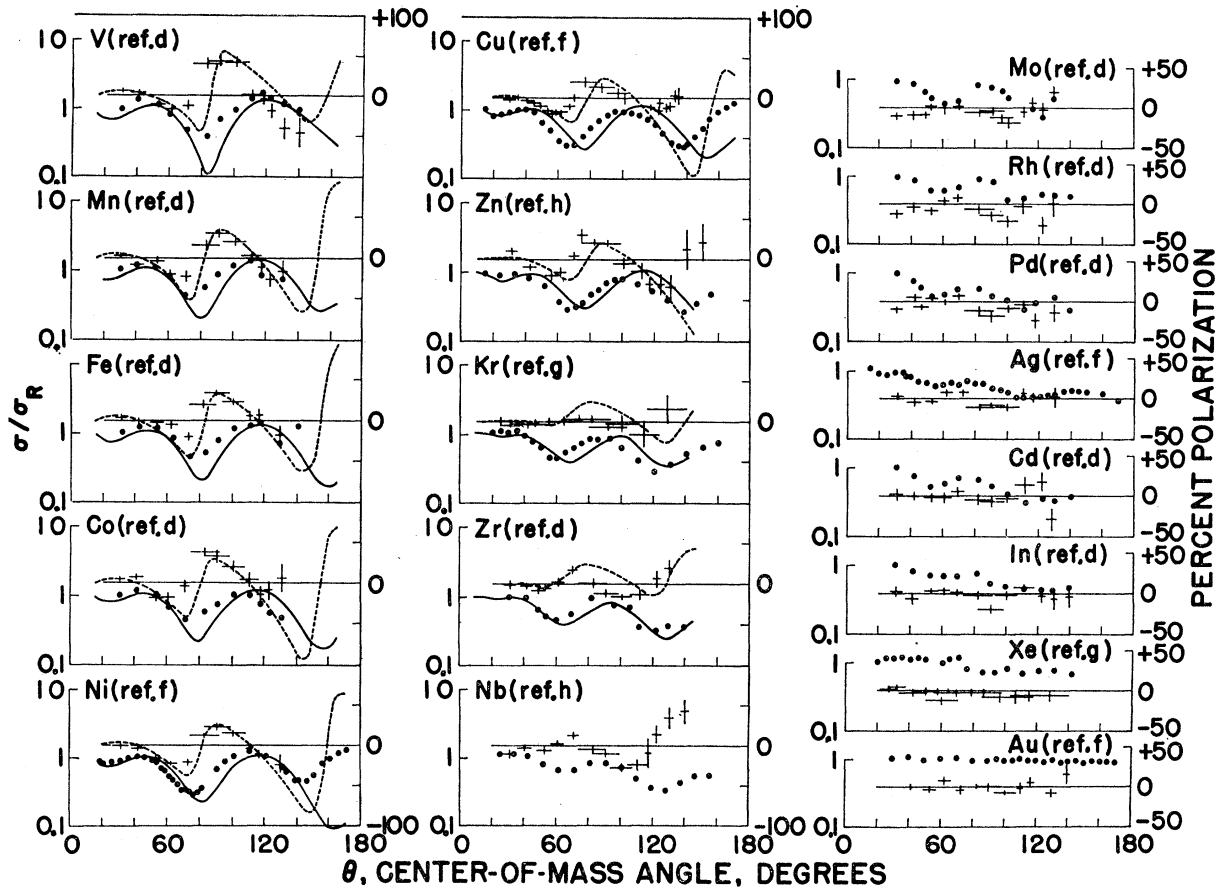[33] L. S. Rodberg, Nuclear Phys. **15**, 72 (1960).

FIG. 5. Angular dependence of the polarization (+) and elastic scattering (•) of protons scattered by various elements. The references are as given in the caption of Fig. 4.

"down" protons) would fall between those for spin "up" and spin "down" protons. One might therefore anticipate strong and oppositely directed polarization effects on either side of the minimum for polarized protons and this is in fact what occurs. Furthermore the polarization is almost always negative to the small-angle side of the diffraction minimum and positive to the large-angle side. This implies that the elastic scattering cross section for spin "up" protons goes through a minimum at a somewhat smaller angle than the corresponding cross section for unpolarized protons. Since moving the diffraction pattern to smaller angles requires an increase in the central potential, we may conclude that the spin-orbit force for protons with spins parallel to their orbital angular momentum is equivalent to enhancing the central potential while the spin-orbit force for protons with opposite spin has the effect of counteracting the central potential, just as in the shell model.

The fits shown in Figs. 4 and 5 are evidence that polarization can be described by a single-particle potential. We expect in such a situation a simple dependence on momentum transfer. On the basis of the simple theory for the diffraction of a plane wave by a completely absorbing sphere of radius R, the differ-

ential elastic scattering cross section is proportional to

$$\left[\frac{J_1(2k_1R \sin(\theta/2))}{2k_1R \sin(\theta/2)}\right]^2,$$

where J_1 is a first order Bessel function. For a given feature of the diffraction pattern, e.g., a maximum or minimum, the argument of J_1 remains constant. We have plotted (Fig. 7) $k_1R \sin(\theta/2)$ (which represents the product of nuclear radius and momentum transfer) vs A for corresponding extremum points in the polarization curves and do indeed find that this quantity does not vary greatly with A for corresponding minima (maximum negative polarization) and maxima in the polarization curves.

Whether or not it is useful to attempt a description of the polarization results in terms of a potential model depends upon the relative importance of the cooperative behavior of the entire nucleus compared to the effects of detailed structure. However, the above results certainly indicate that the polarization depends on some general property of nuclei and serves as a justification for an optical model analysis.[1] As seen from Eq. (14), we used the Woods-Saxon radial dependence for

FIG. 6. Three-dimensional view of the angular dependence of the polarization parametric in radius of the target nucleus.
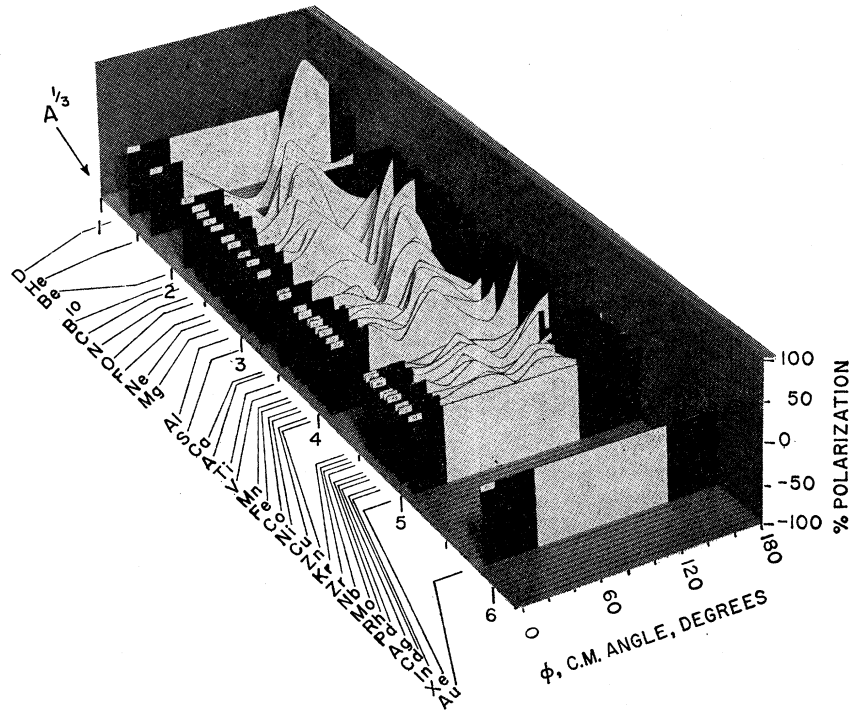
both the real and imaginary parts of the central potential. This radial dependence is relatively constant for $r < R - a$ and goes rapidly to zero with increasing r. It is quite possible that better fits can be obtained by using, for the imaginary part, a surface absorption term as suggested by Bjorklund and Fernbach.[13] The

argument for such a potential is that most of the absorption should occur near the surface where the Pauli exclusion principle is much less effective and the mean free path is correspondingly decreased.[34] Also, surface oscillations will have a higher probability of being induced when the particle is near the surface.

FIG. 7. $k_1 R \sin(\theta/2)$ versus A for positions of corresponding maxima and minima in the polarization curves.

---
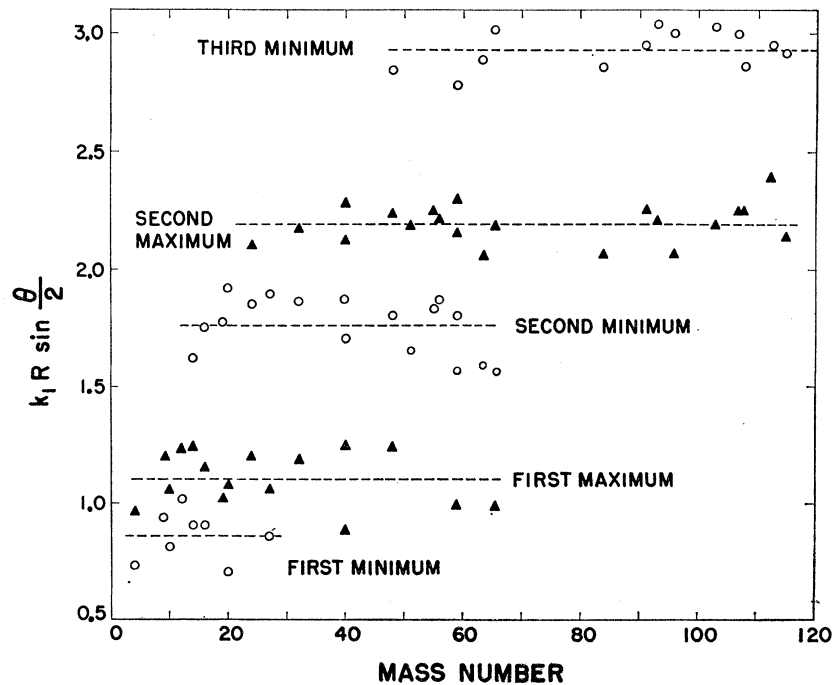
[34] R. H. Lemmer, Th. A. J. Maris, and Y. C. Tang, Nuclear Phys. 12, 619 (1959).

On the other hand, recent calculations by Kikuchi[35] indicate that surface absorption is not overwhelmingly dominant at intermediate energies. Only further calculation (and experiments) can determine the relative merits of the two potentials.

Evaluation of the parameter a in the Woods-Saxon potential permits one to say something about the surface thickness, t, of the nucleus. Defining t as the distance for $V\rho(r)$ to decrease from $0.9V$ to $0.1V$, our value of 0.5 f for a implies a value of 2.2 f for t.

For the spin-orbit energy term we used the usual Thomas-type term proportional to the gradient of the real part of the central potential. Here again better fits can no doubt be obtained by making the spin-orbit term complex, but this too would introduce an additional parameter.

The optical model, representing as it does an energy average of the effect of a nucleus upon an incident particle, is obviously an oversimplification of the actual situation. It is, therefore, not surprising that the theoretical fits to the experimental data do not reproduce all the features of the angular distributions. Among the possible reasons for this disparity as well as for the fluctuations in the angular dependence of the polarization between neighboring elements may be listed the following:

a. Compound Elastic Scattering

This may well be the most serious source of difficulty in the interpretation of the polarization data. Although at the energy of the present experiments the compound nucleus could always decay by neutron emission, we may not have circumvented a significant amount of compound elastic scattering. In fact, there is now evidence that compound elastic scattering may be of considerable importance even at incident energies as high as 10 Mev.[36] Waldorf and Wall,[4] for example, find extensive evidence at 7.5 Mev that compound elastic scattering accounts for an appreciable part of the elastic
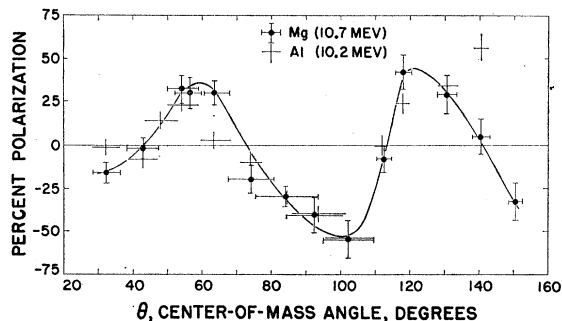
FIG. 8. Comparison of the polarization data for
Mg($I=0$) and Al($I=\frac{5}{2}$).

[35] Ken Kikuchi, Nuclear Phys. 12, 305 (1959).
[36] We are indebted to Professor Alford of the University of Rochester for first pointing this out on the basis of elastic scattering and polarization data which he had taken at 6 and 7 Mev.

scattering cross section, especially at large angles. These authors point out that the relative probability for the compound nucleus to decay through the entrance channel is higher for even A than for odd A elements due to the level structure of the residual nuclei involved. Although a comparison of the angular dependence of polarization for neighboring even A and odd A elements reveals no startling dissimilarities, there are, nonetheless, apparently random fluctuations from a smooth dependence on A which are well outside of experimental uncertainties; and this is especially true at large angles where the elastic scattering cross sections are low and the contribution from compound elastic processes might therefore be relatively large. Whether this is so at 10 Mev and whether other compound nucleus properties are also important will only be deduced from additional experiments in which energy is varied.

b. Spin-spin Interactions

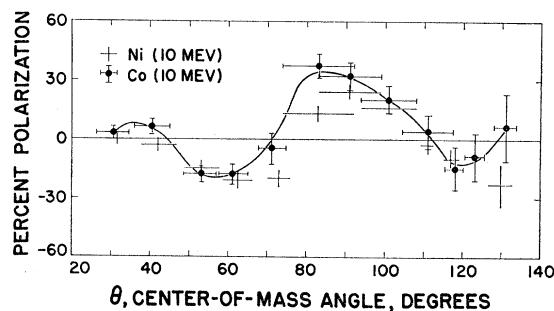These are of course completely neglected in the optical model but their effect should not be large for

FIG. 9. Comparison of the polarization data for
Co($I=\frac{7}{2}$) and Ni($I=0$).

any but the lightest nuclei. There is, for example, very little difference between the polarization from Al($I=\frac{5}{2}$) and from Mg($I=0$) (Fig. 8) or between Co($I=\frac{7}{2}$) and Ni($I=0$) (Fig. 9).

c. Nonspherical Nuclei

The quality of the fits for highly distorted nuclei such as aluminum is not perceptibly worse than for spherical nuclei, so this effect is probably of minor importance.

d. Effect of Symmetry Energy

The symmetry parameter is usually taken proportional to the ratio of the difference and sum of the number of neutrons and protons in the nucleus $(N-Z)/A$. On this point the information is perhaps better than on any of the preceding ones. A comparison is made between the polarization from A^{40} and Ca^{40} (Fig. 10) where the effects of nuclear size, shape, and spin do not enter. Unfortunately the two sets of meas-

urements are not at precisely the same energy. However, it is apparent that the symmetry parameter does not introduce a large perturbation in the polarization distribution although there are differences which seem significant and which energy normalizations do not remove. Here is a case in point where a very precise set of experiments as a function of energy is definitely warranted.

e. Effect of Using Natural Isotopic Mixtures as Targets

Although experiments should certainly be performed with separated isotopes, it would appear from the detailed elastic scattering experiments of Brussel and Williams[4] on the isotopes of Ni and of Beurtey et al.[37] on the Zn isotopes that the present data are not significantly distorted as a result of using natural isotopic mixtures. Also the experiments performed on naturally occurring single isotopes do not yield sharper patterns or qualitatively different magnitudes of polarization than neighboring elements containing several isotopes.

V. CONCLUSIONS

The general conclusions derived from the present work serve to confirm the trends which have been evolving from elastic scattering data.[38]

The existence, as a general phenomenon, of strong polarization effects in proton-nucleus interactions is now beyond question. Both the polarization and elastic scattering data appear to be describable in terms of an optical model. Having assumed such a model, it is then quite obvious that the polarization requires a spin-orbit term in the optical potential, for only then can one account for polarization from spin-zero targets. The spin-orbit interaction is found to depend mainly on the nuclear size and the coupling required is in harmony with the shell model as to both sign and magnitude.

Although double scattering experiments certainly remove some of the ambiguities from the analysis of

[37] R. Beurtey, P. Catillon, R. Chaminade, H. Faraggi, A. Papineau, and J. Thirion, Nuclear Phys. **13**, 397 (1959).

[38] *Proceedings of the International Conference on the Nuclear Optical Model*, Florida State University Studies, No. 32 (Rose Printing Company, Tallahassee, Florida, 1959).
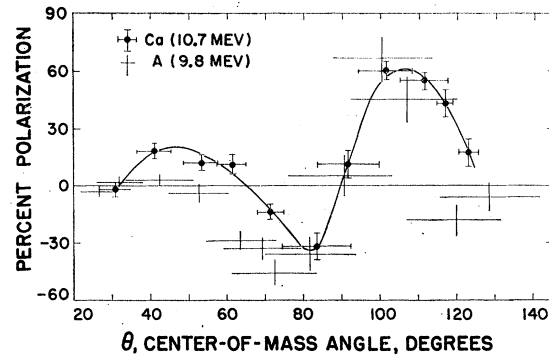

Fig. 10. Comparison of the polarization data for A[40] and Ca[40].

single-scattering data, many uncertainties still remain. Since the optical model describes the reflection, refraction, and absorption of incoming particles, it predicts reaction cross sections as well as the angular dependence of elastic scattering and polarization. So far no data are available on total reaction cross sections and it would appear that without such additional data the optical model parameters will not be uniquely determined.

ACKNOWLEDGMENTS

FIG. 6. Three-dimensional view of the angular dependence of the polarization parametric in radius of the target nucleus.